Quantum Chemical Study of the Mechanism of Reaction between NH ($X\ ^3\Sigma^-$) and H_2, H_2O, and CO_2 under Combustion Conditions

John C. Mackie* and George B. Bacskay

School of Chemistry, University of Sydney, New South Wales 2006, Australia

Received: August 9, 2005; In Final Form: October 23, 2005

Reactions of ground-state NH ($^3\Sigma^-$) radicals with H_2, H_2O, and CO_2 have been investigated quantum chemically, whereby the stationary points of the appropriate reaction potential energy surfaces, that is, reactants, products, intermediates, and transition states, have been identified at the G3//B3LYP level of theory. Reaction between NH and H_2 takes place via a simple abstraction transition state, and the rate coefficient for this reaction as derived from the quantum chemical calculations, $k(NH + H_2) = (1.1 \times 10^{14}) \exp(-20.9\ \text{kcal mol}^{-1}/RT)\ \text{cm}^3\ \text{mol}^{-1}\ \text{s}^{-1}$ between 1000 and 2000 K, is found to be in good agreement with experiment. For reaction between triplet NH and H_2O, no stable intermediates were located on the triplet reaction surface although several stable species were found on the singlet surface. No intersystem crossing seam between triplet NH + H_2O and singlet HNO + H_2 (the products of lowest energy) was found; hence there is no evidence to support the existence of a low-energy pathway to these products. A rate coefficient of $k(NH + H_2O) = (6.1 \times 10^{13}) \exp(-32.8\ \text{kcal mol}^{-1}/RT)\ \text{cm}^3\ \text{mol}^{-1}\ \text{s}^{-1}$ between 1000 and 2000 K for the reaction NH ($^3\Sigma^-$) + $H_2O \rightarrow NH_2$ (^2B) + OH ($^2\Pi$) was derived from the quantum chemical results. The reverse rate coefficient, calculated via the equilibrium constant, is in agreement with values used in modeling the thermal de-NO_x process. For the reaction between triplet NH and CO_2, several stable intermediates on both triplet and singlet reaction surfaces were located. Although a pathway from triplet NH + CO_2 to singlet HNO + CO involving intersystem crossing in an HN−CO_2 adduct was discovered, no pathway of sufficiently low activation energy was discovered to compare with that found in an earlier experiment [Rohrig, M.; Wagner, H. G. *Proc. Combust. Inst.* **1994**, *25*, 993.].

Introduction

Reactions of ground-state NH ($X\ ^3\Sigma^-$) radicals play an important role in combustion processes. NH radicals are key intermediates in the formation of N atoms, and consequently NO, in combustion reactions in air.[1] NH reactions are also important in reburning processes[2] and other techniques such as thermal de-NO_x reactions[3] for reduction of NO from combustion. In the above processes, reaction between NH and H and between NH and NO are the crucial steps. However, ground-state NH ($^3\Sigma^-$) is very reactive with many radicals and molecules present under combustion conditions. Notable among these are reactions between NH and H_2, H_2O, and CO_2. These three reactions were studied by Rohrig and Wagner[4] using NH ($X\ ^3\Sigma^-$) radicals thermally produced from HN_3. Using laser techniques to follow the decay of NH, these workers measured rate coefficients for disappearance of the radicals but did not identify any reaction products. Rohrig and Wagner concluded that each of the above reactions was fast. The values they obtained were $k(NH + H_2) = (1.0 \times 10^{14}) \exp(-20.1\ \text{kcal mol}^{-1}/RT)\ \text{cm}^3\ \text{mol}^{-1}\ \text{s}^{-1}$ (between 1100 and 1800 K), $k(NH + H_2O) = (2.0 \times 10^{13}) \exp(-13.9\ \text{kcal mol}^{-1}/RT)\ \text{cm}^3\ \text{mol}^{-1}\ \text{s}^{-1}$ (between 1300 and 1900 K), and $k(NH + CO_2) = (1.0 \times 10^{13}) \exp(-14.3\ \text{kcal mol}^{-1}/RT)\ \text{cm}^3\ \text{mol}^{-1}\ \text{s}^{-1}$ (between 1200 and 1900 K).

Recently Fontijn et al.[5,6] reinvestigated these three reactions in a high-temperature photochemical reactor, using laser-induced fluorescence from NH to monitor its concentration. Again, no end product analysis was made. Their results for the NH + H_2 reaction were found to be in good agreement with those of Rohrig and Wagner,[4] enabling an extension of the value of $k(NH + H_2)$ to lower temperatures. The combined values of these two groups could be expressed as $k(NH + H_2) = (2.65 \times 10^{13}) \exp(-16.18\ \text{kcal mol}^{-1}/RT)\ \text{cm}^3\ \text{mol}^{-1}\ \text{s}^{-1}$ between 833 and 1685 K. As their rate coefficient for the NH + CO_2 reaction between 415 and 1225 K did not agree with that of Rohrig and Wagner,[4] Fontijn et al.[5,6] have suggested that there might be two distinct reaction mechanisms in the low- and high-temperature regimes. Fontijn et al.[5,6] were also of the opinion that the products of this reaction were not HNO + CO (the products of lowest energy) as suggested earlier,[4] nor were the products of the reaction between NH and H_2O likely to be HNO + H_2 (also the products of lowest energy and, again, the products predicted by Rohrig and Wagner[4]).

In an attempt to elucidate the mechanisms of these three reactions of NH ($X\ ^3\Sigma^-$), we have carried out a detailed investigation of the reaction potential energy surfaces of NH + H_2, NH + H_2O, and NH + CO_2 using quantum chemical techniques.

Theory and Computational Methods

Quantum Chemical Calculations of Thermochemistry. The geometries and energies (and hence heats of formation) of all reactants, products, intermediates, and transition states were determined at the Gaussian-3//B3LYP (G3//B3LYP) level of theory,[7] whereby equilibrium geometries and vibrational frequencies (scaled by 0.96) are obtained by B3LYP/6-31G(d) density functional calculations. Electronic energies are calculated

* Corresponding author: e-mail j.mackie@chem.usyd.edu.au.

10.1021/jp0544585 CCC: $30.25
Published on Web 12/06/2005

by the G3 approach,[8] that is, approximating QCISD(T,FU)/G3Large energies by a QCISD(T)/6-31G(d) calculation plus basis-set corrections evaluated at MP4 and MP2 levels. A higher level correction (based on the number of valence electrons with α and β spins) and spin−orbit corrections applied to open-shell atoms complete the G3//B3LYP protocol.

Reaction Potential Energy Surfaces. Each potential energy surface (PES) was thoroughly investigated at the B3LYP/6-31G(d) level of theory, locating the stationary points corresponding to reactants, products, intermediates, and transition states. In addition, portions of the NH + H_2O surface were characterized by MP2 methods. Where appropriate, the nature of transition states has been confirmed by intrinsic reaction coordinate analysis. The electronic energies at the stationary points on the PES were determined at the G3//B3LYP level of theory, except in the case of singlet biradical species and systems with highly stretched bonds, which require multireference configuration interaction (MRCI) treatments. Spin-unrestricted density functional theory (DFT) (UB3LYP) was found to be a reasonable alternative for such species.

The geometry corresponding to intersystem singlet−triplet crossing of the potential energy surfaces in the case of the HN−CO_2 adduct, defined as the minimum of the crossing seam, was determined at the B3LYP/6-31G(d) level of theory, utilizing the method proposed by Koga and Morokuma.[9] This consists of minimization of the Lagrangian

$$L(\mathbf{R}, \lambda) = E_1(\mathbf{R}) - \lambda[E_3(\mathbf{R}) - E_1(\mathbf{R})] \qquad (1)$$

where $E_1(\mathbf{R})$ and $E_3(\mathbf{R})$ represent the singlet and triplet energies at geometry $\mathbf{R}$ and λ is the Lagrange multiplier. The minimization of $L(\mathbf{R}, \lambda)$ is carried out iteratively, via a Newton−Raphson-type approach where the Lagrangian in each iteration is expanded as a quadratic function of the change in geometry $\Delta\mathbf{R}$. In practice, as discussed in detail by Koga and Morokuma,[9] this requires the computation of first and second geometric derivatives of the singlet and triplet energies.

All DFT and G3//B3LYP calculations were carried out with the Gaussian03[10] package, while the MRCI calculations[11,12] were completed with MOLPRO.[13] The computations were carried out on DEC Alpha 600/5/333 and Compaq XP100/500 workstations of the Theoretical Chemistry group at the University of Sydney and on the Compaq AlphaServer SC system of the Australian Partnership for Advanced Computing National Facility at the National Supercomputing Centre, ANU, Canberra.

Results and Discussion

NH + H_2 Reaction Potential Energy Surface. Results of the G3//B3LYP calculations, viz., total energies (including zero point correction) E_0, atomization energies ΣD_0, enthalpies of formation at 0 K, rotational constants and (scaled) vibrational frequencies of reactants, products, intermediates and transition states for all the reactions studied in this work are summarized in Table 1. No stable intermediates were found on the NH + H_2 triplet PES. The sole transition state located is the abstraction transition state TS1, HN--H--H, for the reaction NH ($^3\Sigma^-$) + H_2 → NH_2 ($^2B_1$) + H (^2S), whose structure is given in Figure 1. The reverse of this reaction, NH_2 + H → NH + H_2, has previously been studied theoretically by two groups.[14,15] Xu et al.[14] investigated this reaction potential energy surface by MP4−SAC (scaling all correlation energy) methods, while Linder et al.[15] employed both complete active space self-consistent field (CASSCF) and MRCI techniques to study this reaction. Optimized geometries of the HN--H--H transition state at MP4−SAC and MRCI/cc-pVDZ levels of theory, respectively, were quite similar to that of TS1 in Figure 1, although the DFT optimization gave a somewhat larger H3−H4 bond length (1.098 Å as opposed to 1.046 Å obtained by MRCI). At 0 K, Xu et al.[14] calculated at their highest level of theory [UMP2(FU)/6-311G**] that NH + H_2 lay 10.77 kcal mol^{-1} below NH_2 + H. Their calculated barrier height in the exothermic direction was 9.05 kcal mol^{-1}. Using the higher level MRCI/cc-pVDZ, Linder et al.[15] calculated the reaction energy to be −12.97 kcal mol^{-1} and the barrier height to be 5.69 kcal mol^{-1} with respect to NH_2 + H. In comparison, from Table 1, our G3//B3LYP results are −13.00 kcal mol^{-1} for the reaction energy and 5.72 kcal mol^{-1} for the barrier height, both results in excellent agreement with those of Linder et al.[15]

Rate Coefficient for the Reaction NH + H_2 → NH_2 + H. With the data of Table 1, a transition-state theory (TST) calculation of this rate coefficient gave k(NH + H_2) = (1.1×10^{14}) exp(−20.9 kcal mol^{-1}/RT) cm^3 mol^{-1} s^{-1} between 1100 and 1800 K, in good agreement with the value reported by Rohrig and Wagner.[4] At 800 K, our value is somewhat lower yet still in reasonable agreement with the lower temperature data of Fontijn et al.[6] Inclusion of tunneling in our TST calculations at temperatures below about 1000 K would be expected to improve the agreement with the lower temperature data. Both Linder et al.[15] and Xu et al.[14] carried out canonical variational transition state (CVT) theory calculations of the rate coefficient of the reverse reaction (NH_2 + H → NH + H_2). As Linder et al. point out, if the potential barrier for the reaction is low and broad, different portions of the potential surface will control the reaction rate at different temperatures. However, they concluded that for the reaction of interest, the barrier (in the exothermic direction) was sufficiently large and peaked that variational effects were small, ranging from about 10% at 2000 K to about 50% at 1000 K. Linder et al.[15] also computed the CVT rate coefficient for the forward reaction to be k(NH + H_2) = (4.44×10^4)$T^{2.62}$ exp(−6861/T) cm^3 mol^{-1} s^{-1}. We compare our computed value with that of Linder et al. and the experimental values of Rohrig and Wagner[4] and Fontijn et al.[6] in Figure 2. Since Xu et al.[14] obtained significantly different thermochemistry from Linder et al. and ourselves, we have not attempted to calculate k(NH + H_2) from their data on the reverse reaction. From Figure 2 we see that there is very good agreement between our computed rate data and the CVT data of Linder et al. and that our conventional transition-state theory calculation only slightly underestimates the rate coefficient in comparison with the CVT value at the lowest temperatures.

However, it is clear from both experiment and theory that the mechanism of the NH + H_2 reaction is a simple H-abstraction.

NH + H_2O Reaction Potential Energy Surface. Energies and molecular constants for the reactants, products, and transition states are given in Table 1. At the unrestricted UB3LYP/6-31G(d) level of theory, the only transition state found on the triplet surface was the relatively high-energy TS2, for a concerted reaction to HNOH + H. Its geometry is given in Figure 1. At this level of theory the hydrogen abstraction reaction to NH_2 ($^2B_1$) + OH ($^2\Pi$) appears to be barrierless. Consequently, variational transition-state theory (vTST)[16,17] was initially used to characterize the transition state. For temperatures between 1300 and 1900 K, density functional theory (B3LYP/6-31G(d)) was used to map the minimum energy path along the potential energy surface as a function of the reaction coordinate (the forming N--H bond at distances between 1.06 and 1.15 Å). The forming N--H bond length was systematically

TABLE 1: G3//B3LYP Total Energies, Atomization Energies, Heats of Formation, Rotational Constants, and Harmonic Vibrational Frequencies of Reactants, Products, Intermediates, and Transition States

	rotational constants, GHz	frequencies, cm^{-1}	E_0/E_h	ΣD_0, kcal mol^{-1}	$\Delta_f H^0_0$, kcal mol^{-1}
NH ($^3\Sigma^-$)	489.5	3108	−55.193 914	80.624	83.53
H_2	1817.9	4275	−1.167 474	103.727	−0.47
HN--H--H, TS1	497.4, 88.6, 75.2	917*i*, 585, 874, 1297, 1568, 3187	−56.331 55	165.628	101.78
NH_2 ($^2B_1$)	678.7, 387.4, 246.6	1537, 3179, 3280	−55.839 579	171.349	44.43
OH ($^2\Pi$)	551.7	3499	−75.696 367	102.275	8.34
H_2O	787.9, 432.3, 279.1	1644, 3579, 3697	−76.383 725	219.162	−56.91
HNO ($^1A'$)	549.1, 42.4, 39.4	1524, 1618, 2707	−130.412 522	197.539	25.60
HNO ($^3A''$)	696.0, 39.7, 37.6	1037, 1539, 3144	−130.383 603	179.392	43.75
HNO(H)--H, TS2	242.0, 20.1, 18.6	1400*i*, 424, 551, 560, 938, 1136, 1320, 3220, 3575	−131.468 743	231.454	94.95
HNH--OH, TS3	246.7, 11.0, 10.8	1893*i*, 206, 371, 578, 1027, 1143, 1699, 3334, 3577	−131.532 361	270.861	55.55[a]
HNOH	293.5, 31.7, 28.6	725, 1081, 1239, 1543, 3211, 3557	−130.999009	251.128	23.64
NH_3O	184.0, 27.3, 27.3	950, 1149, 1149, 1560, 1613, 1613, 2920, 2920, 2963	−131.592 494	309.109	17.29
NH_2OH (trans)	189.2, 25.3, 25.3	394, 904, 1141, 1292, 1380, 1637, 3273, 3360, 3597	−131.633 09	334.583	−8.18
$HNOH_2$	182.0, 19.5, 19.2	311, 456, 603, 688, 1227, 1611, 3204, 3576, 3679	−131.535 728	273.488	52.91
$NH_3O \rightarrow HNO + H_2$, TS4	145.8, 28.2, 26.5	1128*i*, 683, 823, 1117, 1260, 1452, 1600, 2591, 3038	−131.517 078	261.785	64.61
$NH_3O \rightarrow NH_2OH$, TS5	188.8, 23.8, 23.5	1448*i*, 754, 965, 1004, 1189, 1541, 2731, 3311, 3420	−131.554 473	285.250	41.15
$NH_2OH \rightarrow HNOH_2$, TS6	189.3, 19.0, 18.5	688*i*, 493, 529, 762, 1162, 1546, 2999, 3229, 3606	−131.532 364	271.377	55.02
CO_2	11.56	614, 614, 1317, 2339	−188.504 35	383.604	−95.64
CO	56.92	2120	−113.269 97	256.793	−27.82
HN--OCO ($^3A''$), TS7	56.6, 4.64, 4.29	1316*i*, 254, 291, 364, 704, 953, 1146, 1894, 3098	−243.578 688	389.194	62.92
HNOCO ($^3A''$)	76.5, 5.01, 4.70	206, 325, 463, 572, 920, 989, 1437, 1830, 3144	−243.611 202	409.597	42.51
HNO--CO ($^3A''$), TS8	69.5, 4.58, 4.29	618*i*, 141, 306, 486, 527, 1065, 1358, 1931, 3196	−243.604 12	405.153	46.96
$HN-CO_2$ ($^3A''$)	13.4, 11.4, 6.18	392, 419, 471, 625, 955, 1076, 1112, 1404, 3248	−243.652 658	435.611	16.50
HN--CO_2 ($^3A''$), TS9	14.2, 9.94, 5.83	447*i*, 238, 420, 595, 691, 871, 1164, 1915, 3228			17.2[b]
$HN-CO_2$ ($^1A'$)	13.4, 11.7, 6.38	297, 369, 422, 627, 952, 1046, 1084, 1437, 3302			3.05,[c] 1.4[d]
HOC(O)N (^3A)	13.0, 11.3, 6.07	393, 466, 548, 632, 882, 1113, 1280, 1610, 3551	−243.676 63	450.653	1.46
$HN-CO_2$ ($^3A''$) → HOC(O)N, TS10	16.6, 9.84, 6.18	1892*i*, 513, 582, 686, 900, 919, 1039, 1736, 2047	−243.626 962	419.486	32.62
HO--C(O)N, TS11	15.0, 7.60, 5.05	306*i*, 305, 362, 433, 518, 727, 1165, 1977, 3539	−243.614 623	411.743	40.37
NCO	11.58	461, 531, 1248, 1918	−167.924165	313.175	28.31
$HN-CO_2$ ($^3A''$) → HNCO + O(^3P), TS12	13.6, 8.69, 5.34	465*i*, 307, 383, 508, 573, 857, 1175, 2088, 3449	−243.610 423	409.108	43.00
c-O═CON−H (^1A)	24.1, 8.73, 6.55	525, 540, 646, 914, 1042, 1088, 1207, 1974, 3254	−243.693 857	461.463	−9.35
c-O═CON−H → HN(O)CO, TS13	31.9, 6.57, 5.46	400*i*, 342, 378, 498, 894, 1128, 1271, 2235, 3343	−243.644 049	430.208	21.90
HN(O)CO	44.6, 5.46, 4.87	133, 206, 568, 965, 1137, 1387, 2185, 3227	−243.648 246	432.842	19.27
HN(O)--CO, TS14	41.4, 5.06, 4.68	397*i*, 135, 444, 584, 966, 1353, 1451, 1934, 2970	−243.643 868	430.095	22.01
HNCO	857.7, 11.0, 10.8	540, 587, 769, 1284, 2260, 3530	−168.598 775	422.063	−28.94
$HN-CO_2$ ($^1A'$) → *c*-O═CON−H, TS15	13.7, 11.5, 6.40	318*i*, 395, 455, 637, 913, 1052, 1219, 1493, 3286			3.7[e]
$HN-CO_2$($^3A''$) → HN−CO_2 ($^1A'$), TS16	13.6, 11.3, 6.19	203*i*, 417, 499, 610, 938, 1016, 1103, 1435, 3260			17.3[f]
H(^2S)			−0.501 087		51.63[g]
C(^3P)			−37.828 452		169.98[g]
N(^4S)			−54.564 343		112.52[g]
O(^3P)			−75.032 293		58.99[g]

[a] Geometry optimization at UMP2/6-31G(d). Energies were calculated at the G3(MP2) level. [b] Calculated from E_0 values of TS8 and HN−CO_2($^3A''$) evaluated at the UB3LYP//G3Large level. [c] Calculated from E_0 values of HN−CO_2 ($^1A'$) and *c*-O═CON−H evaluated at the UB3LYP//G3Large level. [d] MRCI calculation of triplet−singlet spitting in HN−CO_2. [e] Calculated from E_0 values of TS14 and *c*-O═CON−H evaluated at the UB3LYP//G3Large level. [f] See text. [g] Values from ref 29.

varied while all other geometric parameters were allowed to relax. At each point along the reaction coordinate, the rate coefficient was calculated by canonical transition-state theory at each temperature, thus allowing the geometry that yielded the minimum rate to be identified as the variational transition state. Interestingly, as shown by Xu et al.,[18] a distinct saddle point does exist on this surface at the UMP2 level of theory. The UMP2/6-311G(d,p) calculations of Xu et al.[18] yielded a barrier height of 0.80 kcal mol^{-1} above the products NH_2 + OH. Our G3 calculations, utilizing the UMP2/6-31G(d) saddle point geometry and frequencies (scaled by 0.96), has yielded a barrier of 2.25 kcal mol^{-1}. The geometry of this transition state, TS3, is given in Figure 1. It is very similar to that reported by Xu et al.[18] as well as to the vTST(B3LYP) geometry. We note also that even though no barrier was found at the B3LYP/6-31G(d) level of theory, the G3//B3LYP energy at the vTST geometry obtained at a temperature of 1500 K, is 3.0 kcal mol^{-1} higher than for the NH_2 + OH products, in reasonable agreement with the G3 value of 2.25 kcal mol^{-1}.

It should be noted that because we have located a distinct saddle point with UMP2/6-31G(d) geometry, we have used conventional transition-state theory rather than vTST to calculate the rate coefficients in the following section.

The barrier found in this work (as well as in the earlier study of Xu et al.[18]), or indeed the endothermicity of the reaction leading to NH_2 + OH, are, however, considerably higher (by at least 12 kcal mol^{-1}) than the activation energy deduced by Rohrig and Wagner[4] on the basis of experimental data for the reaction between NH + H_2O. In an effort to find a lower energy pathway, we have also investigated the NH_3O singlet surface in some detail by density functional methods, followed by G3//B3LYP calculations on any intermediates and transition states on this surface. The stable intermediates on the singlet surface include NH_3O (ammonia *N*-oxide), NH_2OH (hydroxylamine), and $HNOH_2$. Transition states located are TS4, for $NH_3O \rightarrow HNO + H_2$, TS5 for $NH_3O \rightarrow NH_2OH$, and TS6 for $NH_2OH \rightarrow HNOH_2$. The last-named species dissociates in a barrierless process to NH ($^1\Delta$) + H_2O. The energies and molecular constants of the singlet-state intermediates and transition states are given in Table 1. Geometries of the transition states are given in Figure 1. A schematic potential energy surface for both triplets and singlets is given in Figure 3.

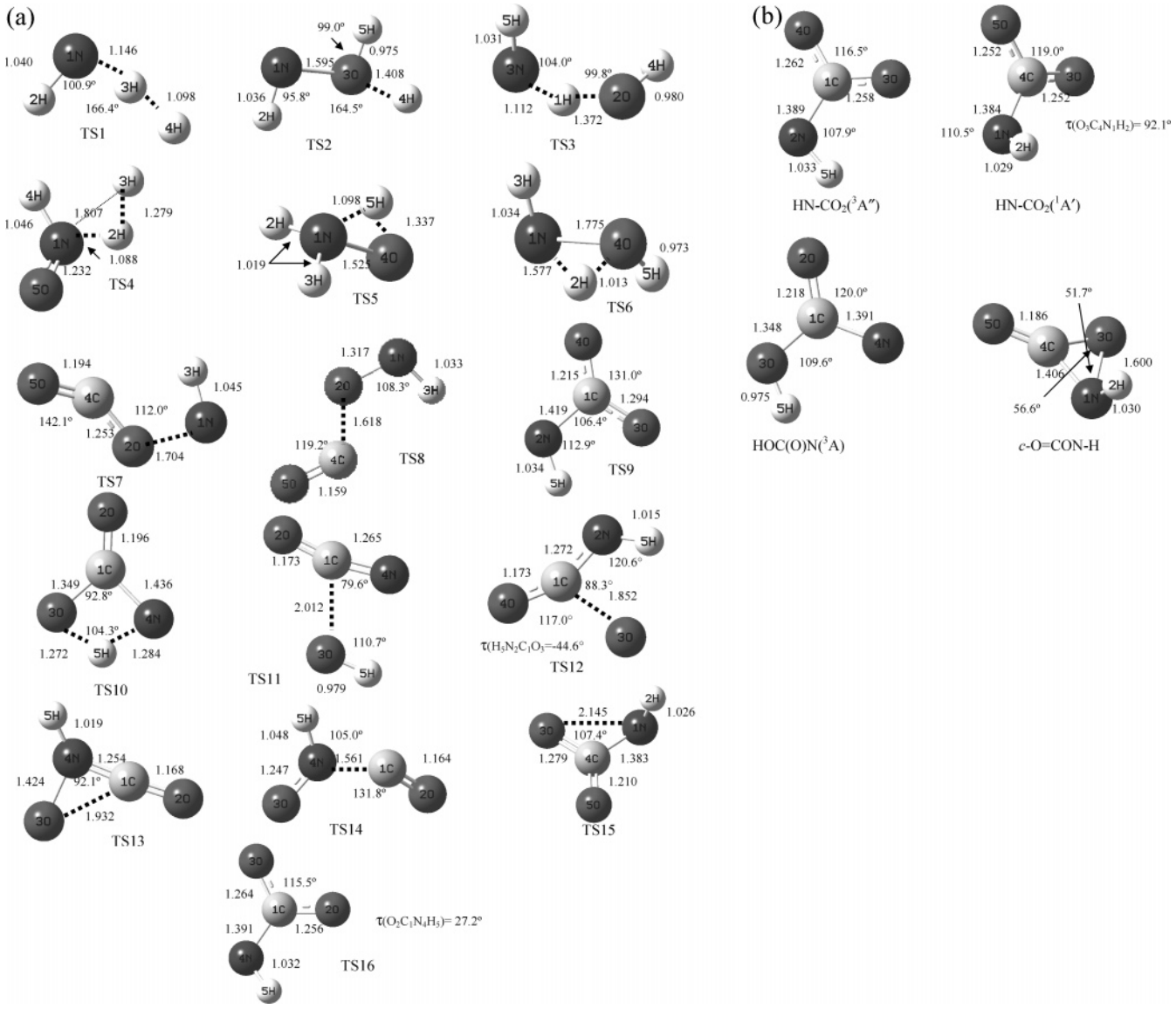

Figure 1. (a) Structures of all transition states on the NH + H_2, NH + H_2O, and NH + CO_2 reaction potential energy surfaces. (b) Selected equilibrium structures on the NH + CO_2 reaction potential energy surface. All bond lengths are given in angstroms.

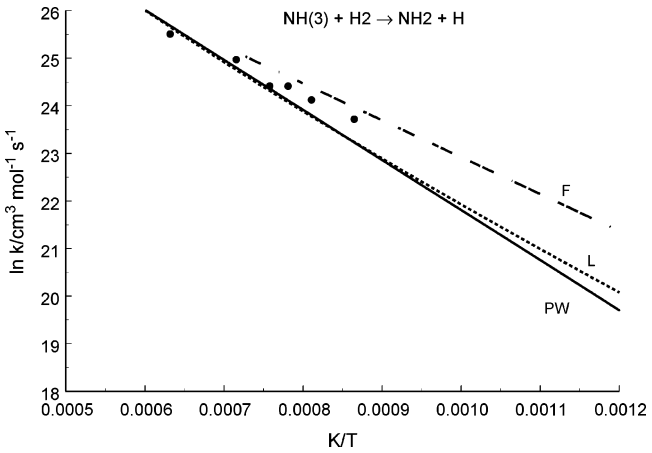

Figure 2. Comparison of theoretical predictions for the rate coefficient for NH + $H_2 \rightarrow NH_2$ + H with experiment. Data points, ref 4; F, experimental dependence from refs 5 and 6; PW, present work; L, ref 15.

In contrast with the singlet species, no stable triplet-state intermediates could be found, nor any intersystem crossing seams between triplet NH + H_2O and singlet HNO + H_2 (the products of lowest energy). We cannot therefore provide quantum chemical evidence to support the contention of Rohrig and Wagner[4] that reaction between ground-state NH and H_2O produces HNO + H_2 by a low-energy pathway.

Rate Coefficient for the Reaction NH + $H_2O \rightarrow NH_2$ + OH. With data from Table 1, including the G3 barrier TS3 located on the triplet surface, the rate coefficient for this reaction calculated by transition-state theory is $k(\mathrm{NH} + \mathrm{H_2O}) = (6.1 \times 10^{13}) \exp(-32.8 \text{ kcal mol}^{-1}/RT) \text{ cm}^3 \text{ mol}^{-1} \text{ s}^{-1}$. On the basis of the data in Table 1, this reaction is endothermic by 26.2 kcal mol^{-1} at 0 K. This, together with the reverse barrier, leads to an activation energy significantly higher than the 13.9 kcal mol^{-1} found by Rohrig and Wagner.[4] Thus, it would appear unlikely that the rate coefficient reported by these workers for reaction between NH and H_2O actually leads to the formation of NH_2 + OH.

The reverse of this reaction is a key reaction in the thermal de-NO_x process,[3] yet little is known experimentally about its reaction rate. In 2000, Dean and Bozzelli[19] made an extensive review of theoretical and experimental data on this reaction. Rate coefficients between 2.5×10^{12} (refs 20 and 21) and 6×10^{12} (ref 22) $\mathrm{cm}^3 \mathrm{mol}^{-1} \mathrm{s}^{-1}$ at 1300 K have been used in

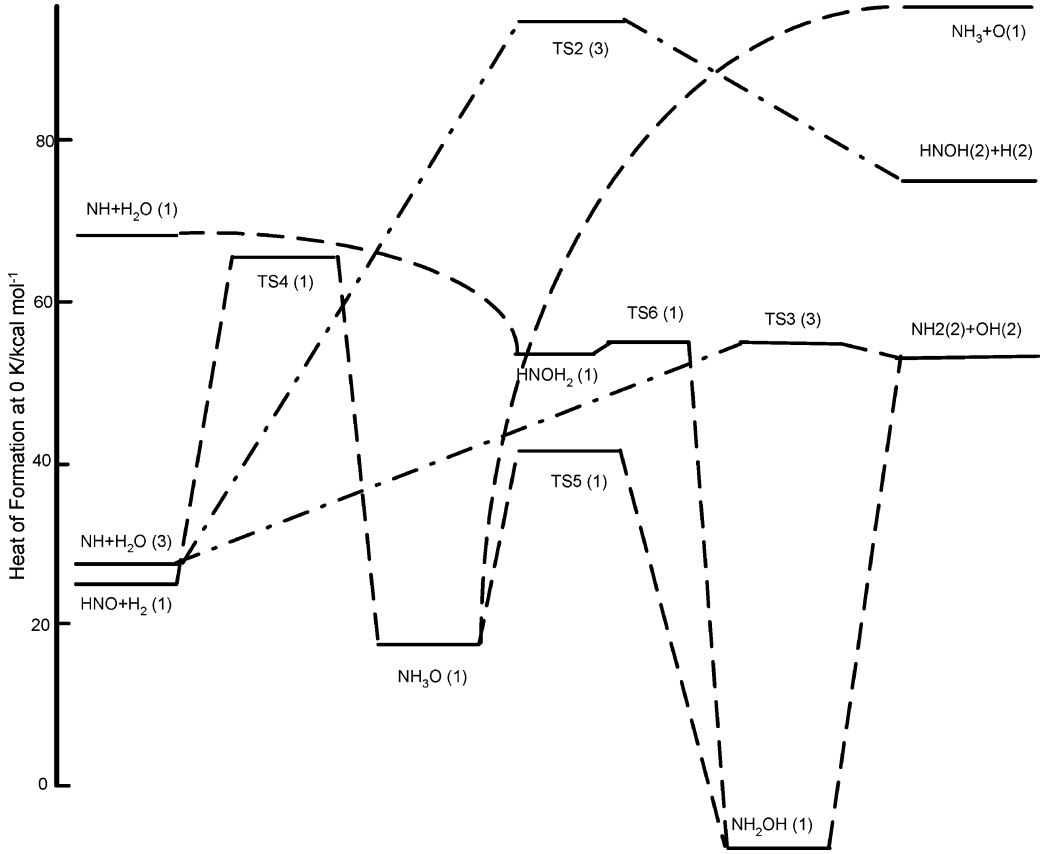

Figure 3. Schematic reaction potential energy surface for reaction between NH($^3\Sigma^-$) and H_2O. Multiplicities are shown in parentheses.

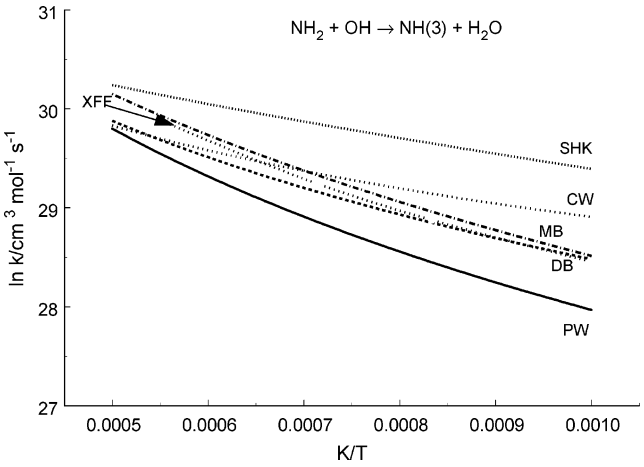

Figure 4. Predicted rate coefficients for $NH_2 + OH \rightarrow NH + H_2O$. PW, present work; SHK, ref 30; CW, ref 23; XFF, ref 18; MB, ref 21; DB, ref 19.

modeling studies. On the basis of a literature review, Cohen and Westberg[23] recommended a value of $(9.0 \times 10^7)T^{1.50}$ exp(460 cal mol^{-1}/*RT*) cm^3 mol^{-1} s^{-1}, which corresponds to 5.0×10^{12} cm^3 mol^{-1} s^{-1} at 1300 K. By use of our ab initio thermochemistry, our calculated rate coefficient for the reaction $NH_2 + OH \rightarrow NH$ ($^3\Sigma$) + H_2O is $k(NH_2 + OH) = (1.64 \times 10^4)T^{2.644}$ cm^3 mol^{-1} s^{-1}, which yields a value at 1300 K of 2.8×10^{12} cm^3 mol^{-1} s^{-1}, in reasonable agreement with previous estimates. In Figure 4, comparison is made with other predictions for the direct hydrogen transfer reaction rate coefficient. While there is agreement between predictions around 2000 K, there is greater uncertainty in lower temperature regions. In comparison with the recommendation of Cohen and Westberg,[23] our two-parameter expression gives a value at 1000 K, which is a factor of about 2.5 less than theirs, while at 2000 K our value is smaller by just 3%.

NH + CO_2 Reaction Potential Energy Surface. The computed energies and molecular constants for the reactants, products, intermediates, and transition states are given in Table 1. As predicted by Fontijn et al.,[5,6] a direct abstraction route to form HNO + CO from NH ($^3\Sigma^-$) + CO_2 is too high-lying. This process takes place in two stages, as shown in Figure 5. First, triplet NH and CO_2 react in an end-on orientation via transition-state TS7 to form the HNOCO (^{3}A″) adduct. The barrier to this process is quite high, namely, 75.0 kcal mol^{-1} above the reactants, as computed by G3//B3LYP. HNOCO can decompose via transition state TS8 to form HNO (^{3}A″) + CO ($^1\Sigma$). Both triplet and singlet $HNCO_2$ reaction potential energy surfaces have been thoroughly investigated by density functional methods with particular emphasis on locating possible low-energy reaction pathways. By use of UB3LYP/6-31G(d) techniques, a stable triplet-state adduct, HN−CO_2, was located. This adduct has C_S symmetry, with all atoms coplanar and an N−C bond of approximately 1.39 Å. At the same level of theory, a transition state for formation of this adduct from NH + CO_2 was located at approximately 1 kcal mol^{-1} higher energy than that of the adduct. The N−C bond in this transition state was computed to be 1.68 Å. However, at the G3//B3LYP level of theory the transition state was found to be 0.5 kcal mol^{-1} lower in energy than the adduct. This suggests that the geometry and energy of the saddle point corresponding to the transition state are very sensitive to the choice of quantum chemical method. The problem is best resolved by computing geometries and energies at the same level of theory (which is not the case when G3//B3LYP and related methods are used). Therefore, we chose to determine the geometries and relative energies of both transition state and stable adduct via UB3LYP/G3Large com-

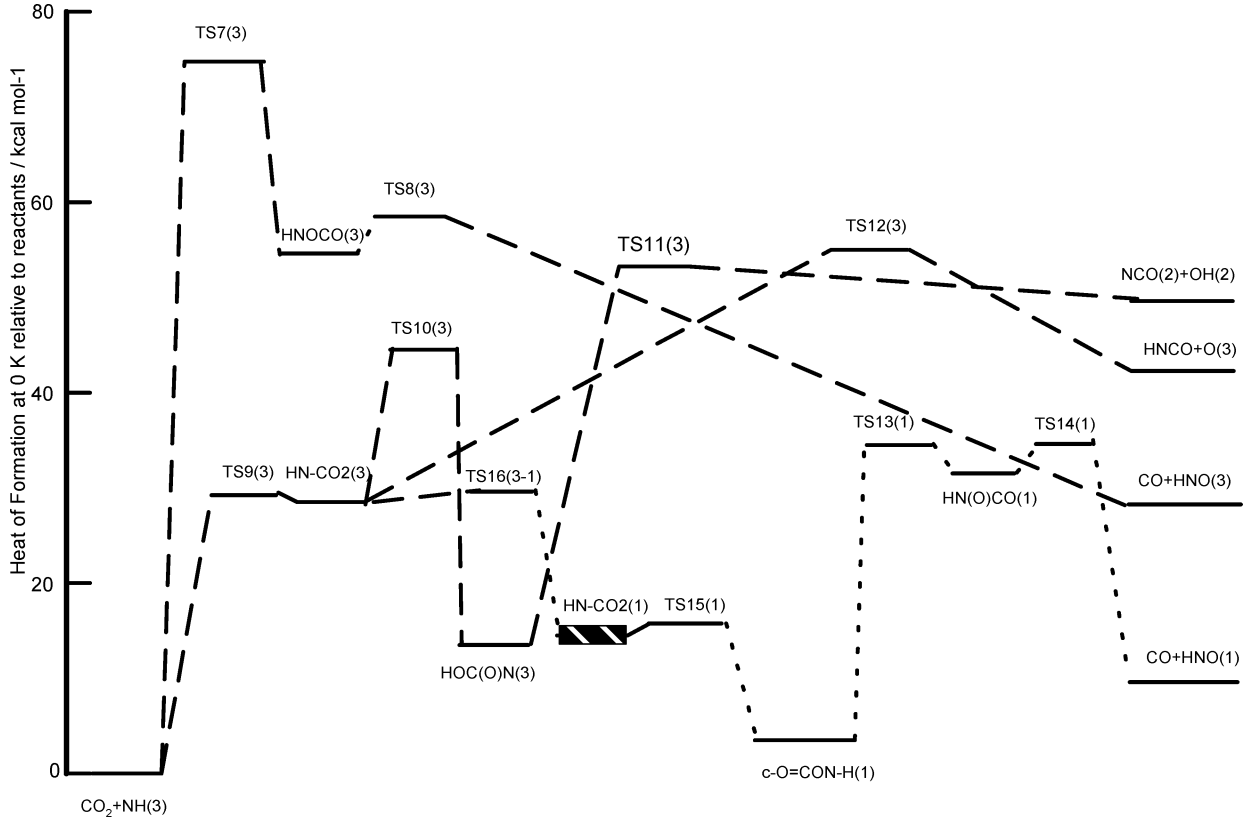

Figure 5. Schematic reaction potential energy surface for reaction between NH($^3\Sigma^-$) and CO_2. Multiplicities are given in parentheses. The shaded region for the HN−CO_2 singlet species represents the uncertainty in energy of this molecule. (See text.)

putations. At this level of theory the transition state, TS9, was found to lie 0.7 kcal mol^{-1} higher than the triplet HN−CO_2 adduct. The structures of these species are shown in Figure 1b. When the (reverse) barrier of 0.7 kcal mol^{-1} is combined with the G3//B3LYP energy of the triplet adduct, the resulting critical energy for the formation of triplet HN−CO_2 (C_S) is 29.3 kcal mol^{-1} above NH ($^3\Sigma^-$) + CO_2.

The triplet HN−CO_2 adduct is not the only equilibrium structure located on the triplet surface. The lowest-lying triplet intermediate was found to be the HOC(O)N species, whose structure is given in Figure 1b. By use of G3//B3LYP, this species was found to lie 13.6 kcal mol^{-1} above the reactants. HOC(O)N can be formed by a 1,3 hydrogen transfer reaction of the HN−CO_2 adduct via transition state TS10, which lies 44.7 kcal mol^{-1} above the reactants. No transition state could be located for the formation of this intermediate from NH ($^3\Sigma^-$) and CO_2 by a one-step concerted reaction. Breaking of the HO−C bond in HOC(O)N leads to the products NCO ($^2\Pi$) + OH ($^2\Pi$) via transition state TS11, which is located at 52.5 kcal mol^{-1} above the reactants. A transition state TS12 has also been found for reaction of the triplet HN−CO_2 to HNCO + O (^{3}P). The barrier for this lies 55.1 kcal mol^{-1} above NH ($^3\Sigma^-$) + CO_2.

Several equilibrium structures have been located on the singlet NH + CO_2 surface. Lowest lying of these is the three-membered cyclic structure O═CON−H at 2.8 kcal mol^{-1} above the reactants NH ($^3\Sigma^-$) + CO_2. Its structure is shown in Figure 1b. There is also an all-planar three-membered ring structure OOC═NH, which lies 32.9 kcal mol^{-1} above the reactants. As this structure presumably correlates with the products HNCO + O ($^1\Delta$), this intermediate was not investigated further. A pathway on the singlet surface has been found from cyclic O═CON−H via TS13 to the open-chain HN(O)−CO intermediate, which in turn passes via TS14 to the products HNO + CO.

A singlet HN−CO_2 adduct, a singlet biradical, was also located. Like the triplet adduct, the singlet structure is of C_S symmetry, but unlike the triplet, singlet HN−CO_2 is not planar: its plane of symmetry is perpendicular to the OCO plane. The bond lengths in the singlet and triplet adducts are very similar and the singlet structure is readily obtained from the triplet's essentially via a rotation of the NH group around the C−N axis. As singlet HN−CO_2 is a biradical, G3-type methods (which utilize single-reference QCI, MP2, and MP4 methods) cannot be used to compute its energy. The most reliable way to characterize singlet biradical species is by MRCI. In the context of this work we used MRCI in conjunction with correlation-consistent basis sets of Dunning and co-workers[24,25] to compute the singlet−triplet separations at the UB3LYP/6-31G(d) geometries of singlet and triplet HN−CO_2, respectively, as well as the adiabatic energy difference between the triplet and singlet states. By use of the aug-cc-pVQZ basis for the MRCI calculations (with a CASSCF reference for two active electrons in two active orbitals and Davidson's correction for quadruple excitations), the adiabatic triplet−singlet energy difference was calculated to be 15.1 kcal mol^{-1}. (At the triplet and singlet geometries the corresponding vertical triplet−singlet separations were computed to be −2.3 and 19.7 kcal mol^{-1}. respectively.) Thus singlet HN−CO_2 is predicted to lie 16.1 kcal mol^{-1} above NH ($^3\Sigma^-$) + CO_2. An alternative simpler approach to estimate the energy of singlet HN−CO_2 is to employ unrestricted (spin-polarized) DFT. In light of the similarities between the singlet HN−CO_2 and cyclic O═CON−H structures, we chose to compute their energy separation at the UB3LYP/G3Large level of theory, which predicted the singlet adduct being 12.4 kcal mol^{-1} above the cyclic intermediate, that is, 14.3 kcal mol^{-1} above NH ($^3\Sigma^-$) + CO_2. The consistency between the DFT and MRCI results is very good. A small barrier

of 0.6 kcal mol^{-1} was found for closure of the N−O bond in the singlet adduct to form the cyclic intermediate via TS15.

The question now arises as to what is the lowest energy pathway from the triplet reactants NH ($^3\Sigma^-$) + CO_2 to the products of lowest energy, viz., the singlet HNO + CO. Initial reaction can produce the triplet HN−CO_2 adduct. The lower-lying singlet adduct would correlate with the higher energy singlet NH + CO_2 (computed by G3//B3LYP to have an energy of 41.8 kcal mol^{-1} with respect to the reactants). However, as the structures of the singlet and triplet adducts are so similar, it seems feasible that triplet−singlet intersystem crossing can take place essentially by the torsion of the N−H group about the C−N bond in the adduct, as indeed suggested by the MRCI calculations discussed above.

The triplet−singlet crossing point, defined as the minimum energy of the crossing seam of the singlet and triplet surfaces, was located by the method of Koga and Morokuma,[9] as summarized in the Theory and Computational Methods section, at the B3LYP/6-31G(d) level of theory. The energy of the resulting crossing point (including zero-point corrections) is 0.78 kcal mol^{-1} above the triplet adduct or 29.4 kcal mol^{-1} above the reactants NH ($^3\Sigma^-$) + CO_2. The geometric structure (where the triplet and singlet states have identical energies) can be regarded as a reasonable approximation to that of the transition state for intersystem crossing (TS16 of Figure 1).

Thus, we predict that the lowest energy pathway on the $HNCO_2$ surface, commencing with the reactants NH ($^3\Sigma^-$) + CO_2, would involve intersystem crossing of a triplet HN−CO_2 adduct to form its singlet counterpart, which would collapse into the stable cyclic O═CON−H intermediate. This process would take place with a barrier of approximately 30 kcal mol^{-1}. Further reaction to end products HNO + CO would require an additional barrier of 34 kcal mol^{-1} from cyclic O═CON−H.

Rate Coefficient for Reaction between NH ($^3\Sigma^-$) + CO_2. In our lowest energy pathway as described above, the reactants lead to a stable well (the cyclic O═CON−H intermediate) via a barrier whose energy is equal to that of the intersystem crossing-point. The intermediate can further react via a barrier of comparable magnitude to form the end products HNO + CO. Since the intermediate HN(O)−CO lies in a very shallow well of depth ∼2.7 kcal mol^{-1} below the maximum barrier to HNO + CO, it is justified to neglect this intermediate in a simplified kinetic analysis. The frequency of crossing the first barrier will depend on, in addition to the partition function of the optimized adduct structure at the intersystem crossing point, the pressure and nature of the collider gas. To further simplify our analysis, we assume that every collision with at least the critical energy will lead to intersystem crossing from triplet to singlet adduct. Hence we simply provide in this analysis a maximum limiting value of the rate coefficient. In this evaluation of the rate coefficient for k(NH + CO_2), there is an initial barrier of 29.4 kcal mol^{-1} to produce the cyclic O═CON−H intermediate. This intermediate occupies a well of depth 26.6 kcal mol^{-1} below the initial barrier and 31.2 kcal mol^{-1} below the exit barrier to HNO + CO. Our model therefore comprises a single well (*c*-O═CON−H) with bimolecular reactants (NH + CO_2) and bimolecular products (HNO + CO). Rate coefficients for reaction between NH and CO_2 to produce O═CON−H and HNO + CO have been computed with the MultiWell suite of programs.[26] We assume that the *c*-O═CON−H intermediate, formed from NH + CO_2, will undergo the reverse reaction at an energy-specific rate coefficient, $k(E)$. The limiting high-pressure rate coefficient for the reverse (dissociation) reaction, $k_{\mathrm{uni},\infty}$, is given by

$$k_{\mathrm{uni},\infty} = \frac{1}{q(T)}\int_{E_0}^{\infty} k(E)\rho(E)\exp(-E/k_{\mathrm{B}}T)\,\mathrm{d}E \qquad (2)$$

where $q(T)$ is the internal partition function of the intermediate calculated at the transition temperature T, $\rho(E)$ is the density of states, and k_{B} is the Boltzmann constant. The lower limit of integration is the critical energy of reaction, E_0. The addition rate coefficient in the high-pressure limit, $k_{\mathrm{add},\infty}$, is obtained from $k_{\mathrm{uni},\infty}$ by detailed balance with the equilibrium constant $K_{\mathrm{c}}(T)$ by

$$k_{\mathrm{add},\infty} = k_{\mathrm{uni},\infty}/K_{\mathrm{c}}(T) \qquad (3)$$

The overall pressure-dependent rate coefficient for stabilization of the intermediate and for formation of the products HNO + CO is obtained from the MultiWell simulations by

$$k_{\mathrm{overall}} = f_{\mathrm{products}}k_{\mathrm{add},\infty} \qquad (4)$$

where f_{products} is the fraction of reaction flux to *c*-O + CON−H or HNO + CO. Additional data required for MultiWell are molecular constants for the two transition states involved and the entrance and exit barrier heights, Lennard-Jones parameters for *c*-O═CON−H and the bath gas (evaluated in the present work for N_2), and collisional energy transfer coefficients. As Lennard-Jones parameters are not available for cyclic O═CON−H, we have estimated these by comparison with similar molecules. Values adopted in the MultiWell simulations were σ = 4.5 Å and ϵ/k_{B} = 300 K. The computed rate data were found not to be very sensitive to this choice of parameters. The weak-collision energy transfer model used was that developed by Luther and co-workers[27] and is described in the MultiWell formulation.[26]

It should be noted that recently Klippenstein and Miller[28] have developed a technique for obtaining product-specific rate coefficients from solutions to the master equation in the general case. Their approach differs from the Monte Carlo-based MultiWell method, and the approach of Klippenstein and Miller is particularly useful for extracting rate coefficients from multiple well problems, especially at high temperatures.

Our MultiWell simulations reveal that, between 1000 and 1500 K, a large majority of the reaction flux from NH + CO_2 forms the stable cyclic intermediate O═CON−H. It is only above 1500 K that significant flux leads to the products HNO + CO. At 2000 K, the rate coefficient for reaction to these two products is approximately half the rate coefficient for reaction to the cyclic intermediate. The simulations also demonstrate that there is significant falloff in reaction rates as the pressure is decreased from 10 000 to 1 Torr. In Figure 6, we show the computed rate coefficients into the two product channels, O═CON−H and HNO + CO, for a pressure of 1 atm in a nitrogen bath gas. Also shown is the high-pressure rate coefficient, $k_{\infty\mathrm{f}} \equiv k$(NH + CO_2), for reaction into both channels. This rate coefficient can be well fitted by the simple Arrhenius expression k(NH + CO_2) = (8.2 × 10^{13}) exp(−34.5 kcal mol^{-1}/RT) cm^3 mol^{-1} s^{-1}.

This value must be considered an upper limit to the value of k(NH + CO_2) as evaluated quantum chemically, since in addition to the requirement of limiting high pressure, it assumes that intersystem crossing is not rate-limiting. Comparing this limiting value with that obtained experimentally by Rohrig and Wagner[4] at a temperature of 1500 K (near the mean of their studied temperature range), we see that our value is approximately 2 orders of magnitude lower than the experimental

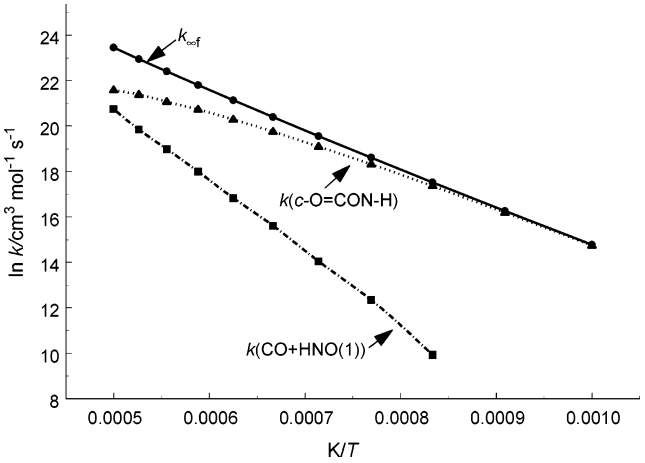

Figure 6. Variation with temperature of the quantum chemical rate coefficients for reaction between NH($^3\Sigma$) and CO_2. Reaction into individual channels at 1 atm pressure is shown together with the high-pressure rate coefficient, $k_{\infty f}$, into both reaction channels.

value. Clearly, the route we have discovered to HNO + CO cannot be the mechanism of the reaction studied by Rohrig and Wagner.

Conclusion

A quantum chemical study of the reaction between NH (X $^3\Sigma^-$) radicals and H_2, H_2O, and CO_2 has enabled the formulation of mechanisms as well as the derivation of rate coefficients for these three reactions. For k(NH + H_2) the rate coefficient derived from quantum chemistry is in good agreement with experiment, indicating that reaction takes place via a simple abstraction transition state. For reaction between NH and H_2O, no route from reactants to the products of lowest energy (HNO + H_2) was discovered. However, the derived rate coefficient for the reaction NH + $H_2O \rightarrow NH_2$ + OH is found to be in agreement with literature values used to model the thermal de-NO_x process.[20−22] In the case of the reaction between NH and CO_2, several stable intermediates have been discovered on the reaction potential energy surface including the cyclic O═CON−H species. A route from the triplet-state reactants to the singlet state products of lowest energy, viz., HNO + CO, involving intersystem crossing has been found. However, the activation energy for reaction via this route was found to be significantly higher than the experimental activation energy for reaction between NH and CO_2.

Acknowledgment. We thank Professor Art Fontijn for stimulating discussions on NH reactions.

References and Notes

(1) Miller, J. A.; Bowman, C. T. *Prog. Energy Combust. Sci.* **1989**, *15*, 287.

(2) Smoot, L. D.; Hill, S. C.; Xu, H. *Prog. Energy Combust. Sci.* **1998**, *24*, 385.

(3) Lyon, R. K. *Environ. Sci. Technol.* **1987**, *21*, 231.

(4) Rohrig, M.; Wagner, H. G. *Proc. Combust. Inst.* **1994**, *25*, 993.

(5) Fontijn, A.; Shamsuddin, S. M.; Marshall, P.; Anderson, W. R. *Chem. Phys. Process. Combust.* **2003**, 1.

(6) Fontijn, A.; Shamsuddin, S. M.; Marshall, P.; Anderson, W. R. *Abstracts Work-in-Progress Posters*; 30th International Symposium on Combustion; The Combustion Institute: Pittsburgh, PA, 2004.

(7) Baboul, A. G.; Curtiss, L. A.; Redfern, P. C.; Raghavachari, K. *J. Chem. Phys.* **1999**, *110*, 7650.

(8) Curtiss, L. A.; Raghavachari, K.; Redfern, P. C.; Rassolov, V.; Pople, J. A. *J. Chem. Phys.* **1998**, *109*, 7764.

(9) Koga, N.; Morokuma, K. *Chem. Phys. Lett.* **1985**, *119*, 371.

(10) Frisch, M. J.; Trucks, G. W.; Schlegel, H. B.; Scuseria, G. E.; Robb, M. A.; Cheeseman, J. R.; Montgomery, J. A., Jr.; Vreven, T.; Kudin, K. N.; Burant, J. C.; Millam, J.; Iyengar, S. S.; Tomasi, J.; Barone, V.; Mennucci, B.; Cossi, M.; Scalmani, G.; Rega, N.; Petersson, G. A.; Nakatsuji, H.; Hada, M.; Ehara, M.; Toyota, K.; Fukuda, R.; Hasegawa, J.; Ishida, M.; Nakajima, T.; Honda, Y.; Kitao, O.; Nakai, H.; Klene, M.; Li, X.; Knox, J. E.; Hratchian, H. P.; Cross, J. B.; Adamo, C.; Jaramillo, J.; Gomperts, R.; Stratmann, R. E.; Yazyev, O.; Austin, A. J.; Cammi, R.; Pomelli, C.; Ochterski, J. W.; Ayala, P. Y.; Morokuma, K.; Voth, G. A.; Salvador, P.; Dannenberg, J. J.; Zakrzewski, V. G.; Dapprich, S.; Daniels, A. D.; Strain, M. C.; Farkas, O.; Malick, D. K.; Rabuck, A. D.; Raghavachari, K.; Foresman, J. B.; Ortiz, J. V.; Cui, Q.; Baboul, A. G.; Clifford, S.; Cioslowski, J.; Stefanov, B. B.; Liu, G.; Liashenko, A.; Piskorz, P.; Komaromi, I.; Martin, R. L.; Fox, D. J.; Keith, T.; Al-Laham, M. A.; Peng, C. Y.; Nanayakkara, A.; Challacombe, M.; Gill, P. M. W.; Johnson, B.; Chen, W.; Wong, M. W.; Gonzalez, C.; Pople, J. A. *Gaussian 03*, Revision B.05; Gaussian, Inc.: Pittsburgh, PA, 2003.

(11) Werner, H.-J.; Knowles, P. J. *J. Chem. Phys.* **1988**, *89*, 5803.

(12) Knowles, P. J.; Werner, H.-J. *Chem. Phys. Lett.* **1988**, *145*, 514.

(13) Amos, R. D.; Bernhardsson, A.; Berning, A.; Celani, P.; Cooper, D. L.; Deegan, M. J. O.; Dobbyn, A. J.; Eckert, F.; Hampel, C.; Hetzer, G.; Knowles, P. J.; Korona, T.; Lindh, R.; Lloyd, A. W.; McNicholas, S. J.; Manby, F. R.; Meyer, W.; Mura, M. E.; Nicklass, A.; Palmieri, P.; Pitzer, R.; Rauhut, G.; Schütz, M.; Schumann, U.; Stoll, H.; Stone, A. J.; Tarroni, R.; Thorsteinsson, T.; Werner, H.-J. MOLPRO: a package of ab initio programs designed by H.-J. Werner and P. J. Knowles; version 2002.6.

(14) Xu, Z.-F.; Fang, D.-C.; Fu, X.-Y. *J. Phys. Chem.* **1995**, *99*, 5889.

(15) Linder, D. P.; Duan, W.; Page, M. *J. Phys. Chem.* **1995**, *99*, 11458.

(16) Hase, W. L.; Mondro, S. L.; Duchovic, R. J.; Hirst, D. M. *J. Am. Chem. Soc.* **1987**, *109*, 2016.

(17) Haworth, N. L.; Bacskay, G. B.; Mackie, J. C. *J. Phys. Chem. A* **2002**, *106*, 1533−1541.

(18) Xu, Z.-F.; Fang, D.-C.; Fu, X.-Y. *Theor. Chem. Acc.* **2000**, *104*, 7.

(19) Dean, A. M.; Bozzelli, J. W. In *Gas-Phase Combustion Chemistry*; Gardiner, W. C., Jr., Ed.; Springer-Verlag New York Inc.: New York, 2000; p 125.

(20) Dean, A. M.; Hardy, J. E.; Lyon, R. K. *Proc. Combust. Inst.* **1982**, *19*, 97.

(21) Miller, J. A.; Bowman, C. T. *Prog. Energy Combust. Sci.* **1989**, *15*, 287.

(22) Kimball-Linne, M. A.; Hanson, R. K. *Combust. Flame* **1986**, *64*, 337.

(23) Cohen, N.; Westberg, K. R. *J. Phys. Chem. Ref. Data* **1991**, *20*, 1211.

(24) Dunning, T. H., Jr. *J. Chem. Phys.* **1989**, *90*, 1007.

(25) Wilson, A. K.; Woon, D. E.; Peterson, K. A.; Dunning, T. H., Jr. *J. Chem. Phys.* **1999**, *110*, 7667 and references therein.

(26) Barker, J. R. MultiWell software, version 1.2.0, 2002; Barker, J. R. *Int. J. Chem. Kinet.* **2001**, *33*, 232.

(27) Hold, U.; Lenzer, T.; Luther, K.; Reihs, K.; Symonds, A. C. *J. Chem. Phys.* **2000**, *112*, 4076.

(28) Klippenstein, S. J.; Miller, J. A. *J. Phys. Chem. A* **2002**, *106*, 9267.

(29) Chase, M. W., Jr. NIST−JANAF Thermochemical Tables, 4th ed. *J. Phys. Chem. Ref. Data* **1998**, Monograph 9.

(30) Salimian, S. S.; Hanson, R. K.; Kruger, C. H. *Combust. Flame* **1984**, *56*, 83.